

Framed Fidelity MAC: Losslessly packing multi-user transmissions in a virtual point-to-point framework

Zhao Li^{a,*}, Bigui Zhang^a, Chengyu Liu^a, Zhixian Chang^b, Kang G. Shin^c, Zheng Yan^{a,d}

^a School of Cyber Engineering, Xidian University, Xi'an 710126, China

^b School of Commun. and Inf. Engineering, Xi'an University of Posts & Telecommun., Xi'an 710061, China

^c Department of Elec. Engineering and Computer Science, The University of Michigan, Ann Arbor 48109, USA

^d The Department of Connet, Aalto University, Espoo 02150, Finland

ARTICLE INFO

Keywords:

Multi-user communication
Medium access control (MAC)
Co-channel interference (CCI)
Interference management (IM)
Spectral efficiency

ABSTRACT

As the number of subscribers in wireless communication systems grows rapidly, it has become important to design efficient medium access control (MAC) protocols to realize resources sharing among multiple users. When designing a MAC, effective management of co-channel interference (CCI) among multiple concurrent transmissions is critical to enhancing system's spectral efficiency (SE). Although MACs based on existing signal processing can suppress/mitigate CCI among multiple concurrent transmissions, they either consume communication resources or attenuate the desired signals' transmission, hence incurring loss of transmission performance. To remedy this deficiency, we propose a *Framed Fidelity MAC* (F^2 MAC) to losslessly pack multi-user data transmissions into a virtual point-to-point (p2p) framework. Under F^2 MAC, the common receiver (Rx) selects a virtual framed-channel (a.k.a. *framework*) and broadcasts it to all mobile terminals. The latter calculate their precoding vectors based on the received virtual framework and their respective communication channels with respect to (w.r.t.) the Rx. Then, the pre-processed signals of multiple users are sent to the Rx via different eigenmodes of the framed-channel. By applying a receive filter to the received mixed signal, Rx can recover users' desired data without interference. Since F^2 MAC can decouple the channel quality information (CQI) from channel direction information (CDI) related to the user's signal transmission, — i.e., CQI is exclusively determined by the user's communication channel while CDI depends on the unified framework, it can avoid the transmission performance loss incurred by existing signal processing based MAC which adjusts both CQI and CDI simultaneously. Moreover, we propose a *Flexible Framed Fidelity MAC* (F^3 MAC) to further improve the system's SE. By dynamically re-constructing the virtual framed-channel at each mobile user, the user's transmission can be realized with the principal eigenmode's gain of his/her communication channel. Our in-depth analysis and simulation results have shown the proposed MAC methods to significantly improve the SE of multi-user communication systems.

1. Introduction

With the development of 5G (The Fifth Generation) and future communication technologies, the number of subscribers and devices connecting to the network has been increasing dramatically, resulting in rapid growth of users' data traffic. To efficiently utilize limited spectrum resources and accommodate more subscribers' data transmissions, medium access control (MAC) has been studied extensively since the birth of mobile communication [1]. Typical MACs can be divided into fixed and random multiple accesses. The former includes Time Division Multiple Access (TDMA), Frequency Division Multiple Access (FDMA), Code Division Multiple Access (CDMA), Space Division Multiple Access (SDMA), etc. These MAC schemes are featured as

Orthogonal Multiple Access (OMA) [2], i.e., interference-free multi-user transmissions are realized by orthogonally dividing and allocating resources to different users. Although OMA can avoid co-channel interference (CCI) among multiple concurrent transmissions, it also reduces the efficiency of resource utilization, hence limiting the improvement of system capacity. Random multiple access allows users to dynamically access communication resources, and hence can improve the flexibility of resource sharing. However, it inevitably incurs collision and conflict when more than one user claim/use the same resource, thus yielding communication outage and resource wasting. Typical random multiple access schemes include ALOHA [3], Carrier Sense Multiple Access (CSMA) [4], Packet Reservation Multiple Access (PRMA) [5], etc.

* Corresponding author.

E-mail address: zli@xidian.edu.cn (Z. Li).

<https://doi.org/10.1016/j.comnet.2022.109425>

Received 21 March 2022; Received in revised form 7 August 2022; Accepted 13 October 2022

Available online 21 October 2022

1389-1286/© 2022 Elsevier B.V. All rights reserved.

Of those OMA schemes, SDMA can distinguish multiple transmissions sharing the same time and frequency resources in spatial domain by employing multiple antennas at both ends of communication link [6]. SDMA is based on the Multi-Input Multi-Output (MIMO) technique, which has been incorporated into international standards of some promising communication systems such as IEEE 802.11ac [7] and Long-Term Evolution Advanced (LTE-A) [8]. Besides, massive MIMO has also become one of the key technologies for 5G. Therefore, research on MIMO-based MAC is of both theoretical and practical significance. In Multi-User MIMO (MU-MIMO) uplink system, signals from multiple mobile terminals are superimposed on each other at their common receiver (Rx); as for downlink MU-MIMO system, the signal perceived by each mobile user contains not only the desired component, but also the undesired signal components intended for the other users. Therefore, for both uplink and downlink multi-user communication systems, signals should be appropriately processed at the transmitter (Tx) and/or Rx so as to avoid CCI, or decoding error will occur in recovering the desired data. In practice, we can pre-process (a.k.a. *precode*) the signals in spatial domain, i.e., adjusting the spatial features of users' signals, so as to coordinate their spatial relationships to mitigate CCI. However, since the spatial channels of mobile users are usually independent of each other, pre-processing will cause spatial mismatch between users' signals and their channels, hence decreasing users' data rate [9]. So, mitigating CCI with less or even no users' transmission performance loss is a challenging issue in the design of MAC and requires a thorough investigation.

Besides, in order to remedy the deficiency of OMA in resource utilization, researchers have proposed numerous Non-Orthogonal Multiple Access (NOMA) techniques, such as Power Domain NOMA (PD-NOMA) [10], Sparse Code Multiple Access (SCMA) [11] and Pattern Division Multiple Access (PDMA) [12], in recent years. Compared to conventional OMA, NOMA can accommodate more subscribers provided with the same amount of spectrum resources, thus improving system spectral efficiency (SE) [13]. However, NOMA needs to eliminate CCI by employing computational expensive signal processing algorithms [14].

Based on the above discussion, effective management of multi-user interference is crucial for MAC design. Typical interference management (IM) methods include Zero-Forcing (ZF) reception [15], Zero-forcing Beamforming (ZFBF) [16], Block Diagonalization (BD), Interference Alignment (IA) [17], and Interference Steering (IS) [18]. Although these IM-based multi-user communication mechanisms can realize interference-free multi-user transmission, they need adjust the spatial features of transmitted signals, thus causing a mismatch between the adjusted signals and their communication channels, e.g., both ZFBF and BD sacrifice individual users' data rate as compared to that achieved in point-to-point MIMO (p2pMIMO) transmission. So, we call such pre-processing schemes *lossy precoding*. Similarly, at the Rx-side, as the receive filter does not match the desired signal, e.g., ZF reception, the user's data rate becomes inferior to that obtained under p2pMIMO. So, we call such post-processing methods *lossy filtering*.

As a comparison, in Singular Value Decomposition (SVD) based p2pMIMO transmission, both precoding and filter vectors match the channel between Tx and Rx, so that single-user channel capacity can be maximized [15]. In practice, channel state information (CSI) consists of channel quality information (CQI) and channel direction information (CDI), indicating the gain and spatial feature of channel and signal transmitted therein, respectively. CDI at the Tx-side (i.e., CDI-Tx) is always used for precoding, while CDI at the Rx-side (i.e., CDI-Rx) can be exploited for determining the filter vector/matrix. Thus, as long as the precoder and receive filter match the channel, the user's transmission can be realized with the gain of his/her own channel (i.e., user's CQI is preserved), achieving *lossless* pre- and post-processing. In essence, existing IM methods modify CDI and CQI simultaneously, hence incurring a mismatch between the user's signal and channel, i.e., loss of transmission gain yields. It is, therefore, important to develop a new

signal processing method that only adjusts CDI while preserving CQI, so that the capacity of multi-user system can be enhanced.

To meet this need, we propose a *Framed Fidelity MAC* (F^2 MAC) for multi-user uplink communications. With F^2 MAC, the common Rx chooses a virtual framed-channel (\mathbf{H}_F). From the decomposition of \mathbf{H}_F we can obtain a left framed-matrix \mathbf{L}_F and a right framed-matrix \mathbf{R}_F . Next, Rx broadcasts \mathbf{H}_F to all Txs (users); each user (say Tx_k) calculates an adjusting matrix based on his/her own transmission channel (\mathbf{H}_k) and the received \mathbf{H}_F . Then, according to \mathbf{R}_F and the adjusting matrix, the precoding vector for Tx_k can be computed. At the Rx, the receive filter for each user's signal is determined based on \mathbf{L}_F . With F^2 MAC, multi-user transmissions can be packed into a framework determined by \mathbf{H}_F , so that they can be simultaneously sent to Rx without interference; this is similar to p2pMIMO where multiple data transmissions are transmitted via a set of decoupled interference-free spatial subchannels. As for Tx_k 's transmission gain, it is exclusively determined by its channel \mathbf{H}_k . That is, F^2 MAC realizes lossless signal processing by only modifying the user's CDI while completely preserving the user's CQI. In addition, we develop an improved version of F^2 MAC by flexibly reconstructing the virtual framework at each Tx before computing the precoding vector, namely *Flexible Framed Fidelity MAC* (F^3 MAC), so as to further improve the system SE.

The main contributions of this paper are two-fold:

- Proposal of *Framed Fidelity MAC* (F^2 MAC) for multi-user uplink communications. By introducing a virtual framed-channel (framework) and calculating the adjusting matrix based on it, the user's precoding vector and the corresponding receive filter at the common Rx are determined. With F^2 MAC, multiple transmissions can be packed into the virtual framework without interference, while the user's transmission gain is exclusively determined by his/her channel.
- Proposal of *Flexible Framed Fidelity MAC* (F^3 MAC). To further improve system SE, each user re-constructs the virtual framework, i.e., the left and right framed-matrices, and designs precoding vector based on the modified framework, then each user's transmission can be realized with the gain of his/her channel's principal eigenmode. This way, system SE can be further improved compared to F^2 MAC.

The rest of the paper is organized as follows. Section 2 gives the related work while Section 3 presents the system model. Section 4 details the design of F^2 MAC and its improved version F^3 MAC. In Section 5, we evaluate the performance of the proposed methods. Finally, we conclude the paper in Section 6.

Throughout this paper, we use the following notations. The set of complex numbers is denoted as \mathbb{C} , while vectors and matrices are represented by bold lower-case and upper-case letters, respectively. Let \mathbf{X}^H and \mathbf{X}^{-1} be the Hermitian (or conjugate transpose) and inverse of matrix \mathbf{X} , respectively. $\|\mathbf{x}\|$ represents the Euclidean norm of vector \mathbf{x} . $\mathbb{E}(\cdot)$ denotes statistical expectation.

2. Related work

In this section, we will present some existing multiple access methods and IM-based multi-user transmission schemes.

2.1. MAC schemes

As is known, the fixed MAC techniques, such as TDMA, FDMA, CDMA and SDMA realize multiple concurrent transmissions by guaranteeing their orthogonality in time, frequency, code and spatial domain, respectively. These methods avoid CCI through orthogonal division of resources. However, due to the limited time and frequency, the number of concurrent transmissions TDMA or FDMA can support is limited. As for CDMA, its capacity is restricted by residual interference among

different users' codes, i.e., a user's received signal-to-interference-plus-noise ratio (SINR) decreases as the number of transmissions grows, thus limiting the system capacity. Moreover, SDMA's capacity depends on the number of antennas at the Tx- and/or Rx-side, which is limited by the complexity and hardware cost of communication equipments.

In order to support more users' data transmissions and meet the demand for high system capacity, design of novel MAC technique is essential. In recent years, researchers have proposed numerous NOMA techniques [10–12]. For example, a NOMA scheme was proposed in [10] for downlink communication, with which the Tx allocates various amounts of transmit power to two mobile users based on their channel qualities — specifically, a smaller (larger) amount of transmit power is allocated to the user with good (poor) channel quality. Signals of different users can then be simultaneously transmitted over the same frequency channel, but CCI occurs. The user with good channel quality first decodes and re-constructs the relatively-strong unintended signal component, and then employs Successive Interference Cancellation (SIC) to subtract the re-constructed signal from the received mixed signal, so as to obtain the desired signal without CCI and recover the information therein. As for the user with poor channel quality, s/he can recover the desired data directly from the received mixed signal owing to the high received SINR. The above NOMA scheme is also regarded as a Power Domain NOMA (PD-NOMA) in [19]. Note that PD-NOMA is also applicable to uplink multi-user systems [20,21]. Besides PD-NOMA, there are other schemes, such as Sparse Code Multiple Access (SCMA) [11] and Pattern Division Multiple Access (PDMA) [12]. With SCMA, sparse codewords of multiple layers of User Equipments (UEs) are overlaid in code and power domains and carried over shared time–frequency resources; the coded bits are directly mapped to multi-dimensional sparse codewords selected from layer-specific SCMA codebooks, hence improving SE with multi-dimensional constellation [11]. Accordingly, the Rx employs a Message Passing Algorithm (MPA) instead of SIC for multi-user detection, but MPA requires an unacceptably high amount of calculation when serious collision happens. The authors of [12] first defined pattern as the mapping of transmitted data to a resource group that may consist of time, frequency, and spatial resources or any combination thereof. Then, the pattern is introduced to differentiate signals of multiple users sharing the same resource. At the Rx-side, SIC is adopted in multi-user detection.

Although NOMA is deemed advantageous over OMA in system capacity, NOMA eliminates CCI at the cost of increasing the complexity of signal processing. Among existing CCI mitigation and multi-user detection methods, the widely used linear detection algorithm, SIC, suffers the error-propagation problem. That is, if an error occurs in the previously detected signal component, the subsequent signal detection will degrade due to the propagation of error [20]. As for the nonlinear detection algorithms, Maximum Likelihood (ML) detection can achieve good multi-user detection performance by inspecting all possible signal combinations and selecting the one that best matches the received signal as the output, but the computational complexity of ML grows exponentially as the number of concurrent users and modulation order increase. The other nonlinear method, i.e., detection based on Maximum A Posteriori (MAP), needs to calculate the Euclidean distance between the symbols carried in the received signal and all of the unintended signals/interferences; the complexity of MAP becomes too high as a large number of users are involved in the system. Although the above two nonlinear detection algorithms can achieve optimal performance in a flat fading channel [14], they are computational expensive; especially when applied to downlink communication system, both methods require mobile users to have strong computational power, hence impeding their practical use.

2.2. IM-based multi-user communication methods

There have been numerous IM methods developed for multi-user communication systems. By pre-processing/precoding at the Tx-side

and/or post-processing/filtering at the Rx-side, IM methods can suppress or eliminate the influence of interferences. Of these methods, ZF reception [15] post-processes the received mixed signal at the interfered Rx with filter vector(s) orthogonal to the interferences, then disturbances to the desired transmission(s) can be mitigated. However, since the spatial feature of ZF filter does not match the desired transmission, the received desired signal suffers power loss. Both IA [17] and ZFBF [16] pre-process signals at the interfering source(s) to make multiple interferences orthogonal to the desired signal(s) at the interfered Rx, which will avoid disturbance to the desired transmission(s). BD [22] suggests that the transmitted signal from base station (BS) intended for a particular mobile station (MS) be restricted to the null space created by the downlink channels associated with all the other users. Therefore, all inter-user interferences within the cell at the MSs can be fully suppressed. However, while IA, ZFBF and BD adjusting the transmitted signals to avoid CCI, they cause mismatch of the signal sent from the interfering Tx to its serving Rx and its transmission channel, hence decreasing the reception gain of the desired signal at the interfering Rx (i.e., Rx associated with the interfering Tx) [16,17,22]. That is, IA, ZFBF and BD realize multi-user communication at the cost of some subscribers' performance loss. In [18], IS constructs a steering signal at the interfered Tx (i.e., Tx corresponding to the interfered Rx) and sends it to the interfered Rx along with the desired signal. This steering signal interacts with, and adjusts the interference into the subspace orthogonal to the desired transmission at the interfered Rx so that the effect of disturbance to the desired transmission is eliminated. However, IS consumes transmit power for generating steering signal, thus under transmit power constraint, power for desired transmission is reduced, incurring performance loss of desired transmission. Moreover, similarly to IA, IS needs to consume a Degree-of-Freedom (DoF), or an antenna, at the interfered Rx for accommodating the adjusted interference(s) [18]; note, however, that such a DoF could be used for desired transmission. Compared to p2pMIMO employing SVD based pre- and post-processing, in which the right and left singular matrices of the channel matrix, acting as CDI-Tx and CDI-Rx, respectively, cooperatively determine the spatial features of sub-channels, either pre-processing with BD and ZFBF, or the post-processing of ZF reception, are lossy.

3. System model

We consider uplink transmission in a multi-user system consisting of K Tx's and one common Rx. Each Tx is equipped with $N_T > 1$ antennas, and the Rx has $N_R > 1$ antennas. Transmit power of each Tx is P_T . There is no collaboration among Tx's. For simplicity, we assume Beamforming (BF) is employed at Tx _{k} ($k \in \{1, 2, \dots, K\}$). The transmitted data of Tx _{k} is x_k , satisfying $\mathbb{E}(\|x_k\|^2) = 1$. All Tx's transmit to Rx simultaneously. The system is assumed to have established ideal synchronization, i.e., signals from Tx's arrive at the Rx at the same time. We use $\mathbf{H}_k \in \mathbb{C}^{N_R \times N_T}$ where $k \in \{1, 2, \dots, K\}$ to denote the channel matrix between Tx _{k} and Rx. We employ a spatially uncorrelated Rayleigh flat fading channel model so that the elements of \mathbf{H}_k are modeled as independent and identically distributed zero-mean unit-variance complex Gaussian random variables. Channels are characterized by block fading, i.e., channel parameters in a block consisting of several successive transmission cycles remain constant in the block and vary randomly between blocks. We assume Tx _{k} can accurately estimate \mathbf{H}_k , and feeds it to Rx via an error-free low-rate link. We assume reliable links for the delivery of CSI and signaling. The delivery delay is negligible relative to the time scale at which the channel state varies.

4. Design of virtual framework based lossless MAC

We first briefly introduce some of typical lossy signal processing methods for multi-user detection, and then detail the design of F²MAC. We will then propose the Flexible F²MAC, or F³MAC, to further improve the system SE. In the end, we will discuss the power overhead and various eigenmode matching methods for the proposed MACs.

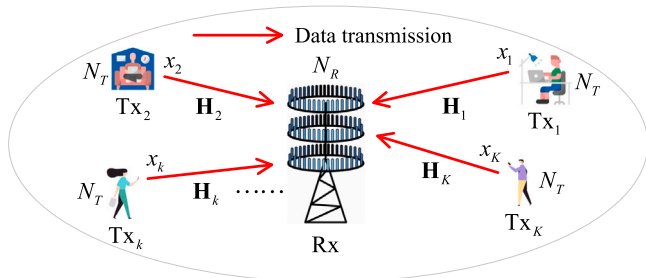


Fig. 1. System model.

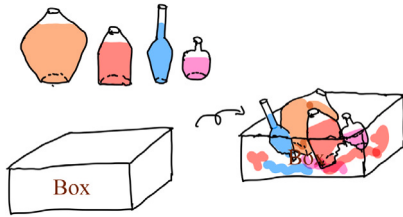


Fig. 2. Illustration of multi-user transmission without IM.

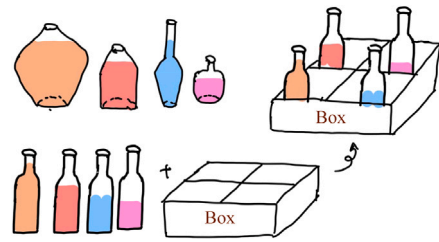


Fig. 3. Illustration of multi-user transmission with lossy signal processing.

Fig. 2 illustrates multi-user transmission without IM. As the figure shows, all of the bottles are directly loaded (i.e., signals without pre-processing) into the box without proper separation (i.e., spatial resource is not properly divided for multi-user transmissions). Then, due to collisions during transportation (i.e., interference among concurrent transmitted signals), the bottles may be broken, hence yielding leakage and mixing different beverages (i.e., interferences are not properly managed). Therefore, at the destination the beverages cannot be received intact; that is, due to bottle damage, only a portion of beverage remaining in the bottle is uncontaminated (i.e., the recovery of desired data is impaired by interferences and hence transmission quality loss occurs).

From Fig. 2 we can see that as CCI is un-managed, signals overlapped with each other at the Rx, so that the quality of multi-user signals' detection deteriorates. In order to manage interference, we can pre-process the signal at Tx. Fig. 3 plots multi-user transmission with lossy signal processing. As the figure shows, by dividing the space of box into multiple grids, collisions among bottles can be avoided (i.e., orthogonality among multiple transmissions is guaranteed). However, since the setting of partitions does not take the beverages' features (i.e., shape and volume) into account, the shape and volume of bottles should be standardized, thus yielding modification of original bottles (i.e., signal quality loss occurs). Owing to the mitigation of collisions among bottles, beverages can be received intactly at their destination. Although the multi-user transmission illustrated in Fig. 3 can avoid CCI, since the spatial channels between users and the Rx are always independent of each other, the adjustment of multiple users' signals is essentially the result of compromising all users. This will cause mismatch of users' signals and their communication channels, hence incurring loss of data rate.

4.1. Introduction to lossy multi-user signal processing

According to the system model given in Fig. 1, we take x_k 's detection as an example without loss of generality. Then, the received signal at Rx can be expressed as:

$$y = \sqrt{P_T} \mathbf{H}_k \mathbf{p}_k x_k + \sum_{i=1, i \neq k}^K \sqrt{P_T} \mathbf{H}_i \mathbf{p}_i x_i + \mathbf{n} \quad (1)$$

where the first term on the right-hand side (RHS) of Eq. (1) is the desired signal, the second term represents the sum of interferences from the other $K - 1$ Txs. \mathbf{p}_i is the precoding vector for x_i at Tx_i . \mathbf{n} is an Additive White Gaussian Noise (AWGN) vector, whose elements have zero mean and variance σ_n^2 . In order to decode x_k , Rx adopts filter vector \mathbf{w}_k to obtain the estimated signal as:

$$\hat{y}_k = \sqrt{P_T} \mathbf{w}_k^H \mathbf{H}_k \mathbf{p}_k x_k + \mathbf{w}_k^H \sum_{i=1, i \neq k}^K \sqrt{P_T} \mathbf{H}_i \mathbf{p}_i x_i + \mathbf{w}_k^H \mathbf{n}. \quad (2)$$

There are two basic reception methods: matched filtering (MF) and ZF reception. With MF, the spatial feature of filter vector \mathbf{w}_k is consistent with that of the signal carrying x_k , and thus \mathbf{w}_k can be determined as $\mathbf{w}_k = \frac{\mathbf{H}_k \mathbf{p}_k}{\|\mathbf{H}_k \mathbf{p}_k\|}$. MF can maximize the receiving power of the desired signal, but the interferences remain un-managed. As for ZF reception, since it cannot guarantee the match of filter vector with the intended signal, resulting in desired signal's power loss, i.e., ZF reception is lossy.

Besides Rx-side filtering, Tx-side precoding can also be employed to realize multi-user communication. For example, ZFBF and BD adjust the spatial features of transmitted signals to avoid CCI. However, with both methods, the spatial features of pre-processed signals no longer match their channels, hence incurring loss of transmission gain. Therefore, both ZFBF and BD are lossy.

To illustrate the basic principle of various signal processing methods, we take beverage transportation as an example. As Fig. 2 shows, there are four types of beverages to be transported. Their shapes and volumes (determined by the bottles) are different from each other, such characteristics can be used to represent the quality of signal transmission. The box used for transportation denotes the spatial channel resource. Then, processing and transmission of multi-user signals can be regarded as packing and transporting multiple types of beverages.

4.2. Design of framed fidelity MAC

Note that in p2pMIMO transmission, multiple signal components are mutually adjusted into orthogonal spatial subchannels (a.k.a. eigenmodes) so as to eliminate CCI. The precoding vectors and receive filters match the transmission channel so that the quality of a signal's transmission is exclusively determined by the eigenmode's gain of the channel. Therefore, the pre- and post- signal processing adopted in p2pMIMO are lossless. In other words, they are featured as *fidelity*. Based on the above observation, F²MAC introduces a virtual framed-channel in the precoding design so that the pre-processed multi-user signals may be sent to Rx via different eigenmodes of the framed-channel. Correspondingly, based on the same framework, Rx designs filter vectors to decode multi-user signals. Then, we can realize lossless signal processing which adjusts spatial features of multi-user signals to avoid CCI while preserving the users' transmission gains. For simplicity, we present the design of F²MAC under $N_T = N_R = K$ in the following discussion.

Under F²MAC, Rx first selects a virtual framed-channel $\mathbf{H}_F \in \mathbb{C}^{N_R \times N_T}$. \mathbf{H}_F can be arbitrarily determined or the same as the user's channel \mathbf{H}_k ($k \in \{1, 2, \dots, K\}$). Applying SVD to \mathbf{H}_F , we can get $\mathbf{H}_F = \mathbf{U}_F \mathbf{D}_F \mathbf{V}_F^H$, the left framed-matrix $\mathbf{L}_F = \mathbf{U}_F$ and right framed-matrix

$\mathbf{R}_F = \mathbf{V}_F$. Then, Rx broadcasts \mathbf{H}_F to all TxS. At the Tx-side, a user, say Tx_k , designs a precoding vector according to the received \mathbf{H}_F and his/her own channel \mathbf{H}_k . Tx_k applies SVD to \mathbf{H}_k to have $\mathbf{H}_k = \mathbf{U}_k \mathbf{D}_k \mathbf{V}_k^H$. Next, Tx_k sets its initial precoding vector to be $\mathbf{r}_F^{(l)}$ ($= \mathbf{v}_F^{(l)}$) where $\mathbf{r}_F^{(l)}$ and $\mathbf{v}_F^{(l)}$ denote the l th column vectors of \mathbf{R}_F and \mathbf{V}_F , respectively; and then designs the adjusting matrix \mathbf{A}_k as $\mathbf{A}_k = \mathbf{H}_k^{-1} \mathbf{L}_F \mathbf{D}_k \mathbf{R}_F^H$; so that the precoding vector can be calculated as $\mathbf{p}_k = \mathbf{A}_k \mathbf{r}_F^{(l)} = \mathbf{A}_k \mathbf{v}_F^{(l)}$. Tx_k employs \mathbf{p}_k as the precoding vector to pre-process its data and sends the processed signal to Rx. Users' signals will propagate along different spatial eigenmodes of \mathbf{H}_F , hence mitigating CCI. Rx adopts the column vectors in \mathbf{L}_F ($= \mathbf{U}_F$) to post-process the received multi-user signals, e.g., by adopting the l th column vector of \mathbf{L}_F , i.e., $\mathbf{l}_F^{(l)}$ ($= \mathbf{u}_F^{(l)}$), which is the l th column of \mathbf{U}_F), as the filter vector \mathbf{w}_k , data x_k can be recovered from the received mixed signal so that multi-user signals can be detected without interference while preserving the gain of each user's transmission over his/her own channel \mathbf{H}_k .

In what follows, we will elaborate on F²MAC's elimination of CCI and realization of multi-user transmissions via mathematical modeling and derivation. Without loss of generality, we let Tx_i ($i \in \{1, 2, \dots, K\}$) adopt the i th column vector of \mathbf{R}_F , i.e., $\mathbf{v}_F^{(i)}$, as the initial precoder. By substituting the precoding vector $\mathbf{p}_i = \mathbf{A}_i \mathbf{r}_F^{(i)} = \mathbf{A}_i \mathbf{v}_F^{(i)}$ and adjusting matrix $\mathbf{A}_i = \mathbf{H}_i^{-1} \mathbf{L}_F \mathbf{D}_i \mathbf{R}_F^H$ into Eq. (1), we can get the received signal at Rx as:

$$\begin{aligned} \mathbf{y} &= \sqrt{P_T} \mathbf{H}_k \left[\mathbf{H}_k^{-1} \mathbf{L}_F \mathbf{D}_k \mathbf{R}_F^H \mathbf{v}_F^{(k)} \right] x_k \\ &+ \sum_{i=1, i \neq k}^K \sqrt{P_T} \mathbf{H}_k \left[\mathbf{H}_k^{-1} \mathbf{L}_F \mathbf{D}_i \mathbf{R}_F^H \mathbf{v}_F^{(i)} \right] x_i + \mathbf{n} \\ &= \sqrt{P_T} \mathbf{U}_F \mathbf{D}_k \mathbf{V}_F^H \mathbf{v}_F^{(k)} x_k + \sum_{i=1, i \neq k}^K \sqrt{P_T} \mathbf{U}_F \mathbf{D}_i \mathbf{V}_F^H \mathbf{v}_F^{(i)} x_i + \mathbf{n} \end{aligned} \quad (3)$$

Take the decoding of Tx_k 's data x_k as an example. Let Rx select the k th column vector of \mathbf{L}_F ($= \mathbf{U}_F$), i.e., $\mathbf{l}_F^{(k)}$ ($= \mathbf{u}_F^{(k)}$), as the receive filter. Then, by applying $\mathbf{w}_k = \mathbf{l}_F^{(k)} = \mathbf{u}_F^{(k)}$ to detecting \mathbf{y} , we can obtain the estimated signal as:

$$\begin{aligned} \hat{y}_k &= \sqrt{P_T} [\mathbf{u}_F^{(k)}]^H \mathbf{U}_F \mathbf{D}_k \mathbf{V}_F^H \mathbf{v}_F^{(k)} x_k \\ &+ \sum_{i=1, i \neq k}^K \sqrt{P_T} [\mathbf{u}_F^{(k)}]^H \mathbf{U}_F \mathbf{D}_i \mathbf{V}_F^H \mathbf{v}_F^{(i)} x_i + [\mathbf{u}_F^{(k)}]^H \mathbf{n} \end{aligned} \quad (4)$$

Since the second term on the RHS of Eq. (4) is zero, we can derive \hat{y}_k as:

$$\begin{aligned} \hat{y}_k &= \sqrt{P_T} [\mathbf{u}_F^{(k)}]^H \mathbf{U}_F \mathbf{D}_k \mathbf{V}_F^H \mathbf{v}_F^{(k)} x_k + [\mathbf{u}_F^{(k)}]^H \mathbf{n} \\ &= \sqrt{P_T} \mathbf{e}^{(k)} \text{diag} \left([\lambda_k^{(1)} \dots \lambda_k^{(k)} \dots \lambda_k^{(K)}] \right) [\mathbf{e}^{(k)}]^T x_k + [\mathbf{u}_F^{(k)}]^H \mathbf{n} \\ &= \sqrt{P_T} \lambda_k^{(k)} x_k + [\mathbf{u}_F^{(k)}]^H \mathbf{n} \end{aligned} \quad (5)$$

where $\mathbf{e}^{(k)}$ is a unit vector whose k th element is 1 and the others are 0, i.e., $\mathbf{e}^{(k)} = [0^{(1)} \dots 0^{(k-1)} 1^{(k)} 0^{(k+1)} \dots 0^{(K)}]$. $\text{diag}(\cdot)$ represents for diagonalization of a vector. We can see from Eq. (5) that after filtering the received signal with \mathbf{w}_k , interference is completely eliminated. Moreover, the gain of desired data x_k is identical to that of the k th eigenmode of Tx_k 's channel \mathbf{H}_k , i.e., $\lambda_k^{(k)}$. In other words, with the above signal processing, the k th main diagonal element of \mathbf{D}_k , i.e., $\lambda_k^{(k)}$, indicating the amplitude gain (i.e., CQI) of \mathbf{H}_k 's k th eigenmode, is embedded into the k th eigenmode of the virtual framework \mathbf{H}_F to replace its k th gain $\lambda_F^{(k)}$ which is the k th main diagonal element of \mathbf{D}_F .

Furthermore, we can present the decoding of K signals in an integral manner as follows. For simplicity, we omit the noise term in the following derivations.

$$\mathbf{Y} = \sum_{i=1}^K \mathbf{H}_i \mathbf{A}_i \mathbf{v}_F^{(i)} x_i. \quad (6)$$

Substituting $\mathbf{A}_i = \mathbf{H}_i^{-1} \mathbf{L}_F \mathbf{D}_i \mathbf{R}_F^H$, $\mathbf{L}_F = \mathbf{U}_F$, and $\mathbf{R}_F = \mathbf{V}_F$ into Eq. (6), we get:

$$\begin{aligned} \mathbf{Y} &= \sum_{i=1}^K \mathbf{U}_F \mathbf{D}_i \mathbf{V}_F^H \mathbf{v}_F^{(i)} x_i = \sum_{i=1}^K \mathbf{U}_F \mathbf{D}_i [\mathbf{e}^{(i)}]^T x_i \\ &= \mathbf{U}_F \text{diag} \left([\lambda_1^{(1)} \dots \lambda_k^{(k)} \dots \lambda_K^{(K)}] \right) \mathbf{x} \end{aligned} \quad (7)$$

where $\mathbf{e}^{(i)} = [0^{(1)} \dots 1^{(i)} \dots 0^{(K)}]$ and $\mathbf{x} = [x_1 \ x_2 \ \dots \ x_K]^T$ is the transmitted data vector consisting of the data of K TxS. We define initial precoding matrix $\tilde{\mathbf{P}} = [\mathbf{v}_F^{(1)} \ \mathbf{v}_F^{(2)} \ \dots \ \mathbf{v}_F^{(K)}]$. Since $\mathbf{V}_F^H \tilde{\mathbf{P}} = \mathbf{E}$ holds where \mathbf{E} is identity matrix, Eq. (7) can be rewritten as:

$$\begin{aligned} \mathbf{Y} &= \mathbf{U}_F \text{diag} \left([\lambda_1^{(1)} \dots \lambda_k^{(k)} \dots \lambda_K^{(K)}] \right) \mathbf{E} \mathbf{x} \\ &= \mathbf{U}_F \text{diag} \left([\lambda_1^{(1)} \dots \lambda_k^{(k)} \dots \lambda_K^{(K)}] \right) \mathbf{V}_F^H \tilde{\mathbf{P}} \mathbf{x}. \end{aligned} \quad (8)$$

We can see from Eq. (8) that with F²MAC, the pre-processed K users' signals are sent to Rx via different eigenmodes of \mathbf{H}_F whose CQI (i.e., $\lambda_F^{(1)}, \dots, \lambda_F^{(K)}$) is replaced by the K users' CQI (i.e., $\lambda_1^{(1)}, \dots, \lambda_K^{(K)}$). Specifically, Tx_k 's transmission quality depends on the gain of \mathbf{H}_k 's k th eigenmode, while its spatial feature is determined by the left and right framed-matrices \mathbf{L}_F and \mathbf{R}_F cooperatively.

We now compare the above derivation with p2pMIMO. According to the descriptions of p2pMIMO in [18], applying SVD to the channel between Tx and Rx, i.e., $\mathbf{H}_{p2p} \in \mathbb{C}^{N_R \times N_T}$, we can have $\mathbf{H}_{p2p} = \mathbf{U}_{p2p} \mathbf{D}_{p2p} \mathbf{V}_{p2p}^H$; then we adopt $\mathbf{P}_{p2p} = [\mathbf{v}_{p2p}^{(1)} \ \mathbf{v}_{p2p}^{(2)} \ \dots \ \mathbf{v}_{p2p}^{(\min(N_T, N_R))}]$ and $\mathbf{W}_{p2p} = [\mathbf{u}_{p2p}^{(1)} \ \mathbf{u}_{p2p}^{(2)} \ \dots \ \mathbf{u}_{p2p}^{(\min(N_T, N_R))}]$ as the precoding and filtering matrices, respectively. Thus, similarly to Eq. (8), we can get the received signal matrix at Rx as:

$$\begin{aligned} \mathbf{Y}_{p2p} &= \mathbf{H}_{p2p} \mathbf{P}_{p2p} \mathbf{x} \\ &= \mathbf{U}_{p2p} \text{diag} \left([\lambda_{p2p}^{(1)} \dots \lambda_{p2p}^{(\min(N_R, N_T))}] \right) \mathbf{V}_{p2p}^H \mathbf{P}_{p2p} \mathbf{x}. \end{aligned} \quad (9)$$

By comparing Eqs. (8) and (9), we can easily see that both equations are very similar. The only difference is that under p2pMIMO the gains of multiple transmissions are from one channel, \mathbf{H}_{p2p} , whereas for F²MAC, $\text{diag} \left([\lambda_1^{(1)} \dots \lambda_k^{(k)} \dots \lambda_K^{(K)}] \right)$ is composed of the gains from K users' channels.

We adopt the filter matrix $\mathbf{W} = [\mathbf{u}_F^{(1)} \ \mathbf{u}_F^{(2)} \ \dots \ \mathbf{u}_F^{(K)}]$ to post-process the mixed signal (given in Eq. (8)), and can obtain:

$$\begin{aligned} \hat{\mathbf{Y}} &= \mathbf{W}^H \mathbf{Y} = \text{diag} \left([\lambda_1^{(1)} \dots \lambda_k^{(k)} \dots \lambda_K^{(K)}] \right) \mathbf{x} \\ &= [\lambda_1^{(1)} x_1 \ \dots \ \lambda_k^{(k)} x_k \ \dots \ \lambda_K^{(K)} x_K]^T. \end{aligned} \quad (10)$$

We can see from Eq. (10) that Rx decodes the signals of K users without CCI, while the transmission gain of each user is exclusively determined by its communication channel. That is, F²MAC realizes lossless signal processing. It should be noted that in the implementation of F²MAC, Rx needs to notify each user the index of \mathbf{R}_F ($= \mathbf{V}_F$) for precoding design; accordingly, such index also determines the receive filter selected from \mathbf{L}_F ($= \mathbf{U}_F$). Multiple TxS are differentiated by using different indices. It can be easily seen that the system SE of F²MAC is the sum of individual users' SE obtained under p2pMIMO mode.

Fig. 4 illustrates the lossless multi-user signal transmission based on the virtual framework. As the figure shows, we divide the box into multiple separating grids of different sizes (representing for different eigenmodes of the virtual framework). Then, in order to pack the beverages into the box, we need to select proper sizes of bottles so as to adapt to various grids (i.e., Tx_k 's transmission quality is determined by the gain of \mathbf{H}_k 's k th eigenmode), so that the shapes of the bottles are preserved, and there is no collision and beverage wasting during transportation (i.e., no transmission quality loss occurs).

Based the above discussion, F²MAC selects a virtual framework to standardize/normalize the transmitted signals. By adjusting multi-user signals into the spatial eigenmodes determined by the framework, the orthogonality of signals is guaranteed. Moreover, since F²MAC

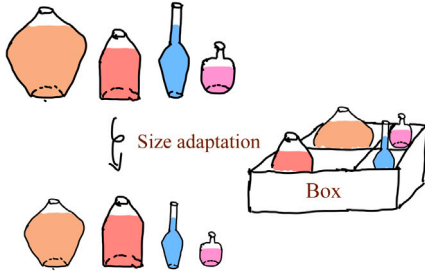


Fig. 4. Illustration of virtual framework based lossless multi-user transmission (i.e., F²MAC).

decouples the signal's transmission quality (i.e., CQI) from its spatial feature (i.e., CDI), the signal's transmission gain is determined by its channel which can be preserved after filtering. However, it should be noted that under F²MAC, only one user can acquire his/her principal eigenmode's gain, whereas the other $K-1$ users can only preserve their non-principal/secondary eigenmodes' gains. Since all of these preserved gains are not degenerated by signal processing, F²MAC has the fidelity (lossless) feature.

4.3. Design of flexible framed fidelity MAC

In the design of F²MAC given in Section 4.2, Tx_k transmits signal/data to Rx via the k th spatial eigenmode of \mathbf{H}_F . Rx recovers data x_k of Tx_k with the k th eigenmode's gain of Tx_k's channel \mathbf{H}_k , i.e., $\lambda_k^{(k)}$. As the gain of \mathbf{H}_k 's eigenmode decreases with the growth of index k , a user with a larger index can only get a smaller gain of his/her channel (i.e., the shapes of the bottles in Fig. 4 remain unchanged, but in order to adapt to the grids of the box, we have to use smaller bottles for some beverages). To solve such a *non-optimal eigenmode's gain preservation problem*, we propose *Flexible Framed Fidelity MAC* (F³MAC). By dynamically re-constructing $\mathbf{R}_F (= \mathbf{V}_F)$ and $\mathbf{L}_F (= \mathbf{U}_F)$ at each Tx, all users can preserve the principal eigenmodes' gains of their communication channels.

We still take Tx_k's transmission as an example. With F³MAC, each Tx first applies SVD to the received \mathbf{H}_F to obtain $\mathbf{R}_F = \mathbf{V}_F$ and $\mathbf{L}_F = \mathbf{U}_F$, and then re-constructs \mathbf{R}_F and \mathbf{L}_F by exchanging the 1st and k th column vectors in \mathbf{R}_F and \mathbf{L}_F , respectively. We define $\mathbf{E}(1, k)$ as a matrix obtained by exchanging the 1st and k th column vectors of an identity matrix \mathbf{E} . Then, by right-multiplying \mathbf{R}_F and \mathbf{L}_F with $\mathbf{E}(1, k)$, respectively, we can obtain the re-constructed left and right framed-matrices \mathbf{R}_{Fk} and \mathbf{L}_{Fk} as:

$$\mathbf{R}_{Fk} = \mathbf{R}_F \mathbf{E}(1, k) = \begin{bmatrix} \mathbf{v}_F^{(k)} & \mathbf{v}_F^{(2)} & \cdots & \mathbf{v}_F^{(1)} & \cdots & \mathbf{v}_F^{(K)} \end{bmatrix} \quad (11)$$

and

$$\mathbf{L}_{Fk} = \mathbf{L}_F \mathbf{E}(1, k) = \begin{bmatrix} \mathbf{u}_F^{(k)} & \mathbf{u}_F^{(2)} & \cdots & \mathbf{u}_F^{(1)} & \cdots & \mathbf{u}_F^{(K)} \end{bmatrix}. \quad (12)$$

Since we have re-constructed \mathbf{R}_F and \mathbf{L}_F , we need to re-calculate the adjusting matrix and precoding vector based on \mathbf{R}_{Fk} and \mathbf{L}_{Fk} following $\mathbf{A}_k = \mathbf{H}_k^{-1} \mathbf{L}_{Fk} \mathbf{D}_k \mathbf{R}_{Fk}^H$ and $\mathbf{p}_k = \mathbf{A}_k \mathbf{r}_{Fk}^{(1)}$, respectively, where the initial precoder $\mathbf{r}_{Fk}^{(1)}$ is the 1st column vector of \mathbf{R}_{Fk} and according to Eq. (11) we have $\mathbf{r}_{Fk}^{(1)} = \mathbf{v}_F^{(k)}$. Substituting $\mathbf{p}_k = \mathbf{A}_k \mathbf{r}_{Fk}^{(1)}$ into Eq. (1), we can get a result similar to that of Eq. (3); the only difference is that in Eq. (3) precoding vector for each Tx is computed according to \mathbf{R}_F and \mathbf{L}_F , whereas under F³MAC, each user determines his/her precoder in terms of the re-constructed framed-matrices \mathbf{R}_{Fk} and \mathbf{L}_{Fk} .

At Rx, we employ $\mathbf{w}_k = \mathbf{l}_{Fk}^{(1)}$ where $\mathbf{l}_{Fk}^{(1)}$ is the 1st column vector of \mathbf{L}_{Fk} , as the filter vector to recover Tx_k's data. From Eq. (12), we have $\mathbf{l}_{Fk}^{(1)} = \mathbf{u}_F^{(k)}$. Then, adopting $\mathbf{w}_k = \mathbf{l}_{Fk}^{(1)}$ to process the received mixed signal can output a result similar to that of Eqs. (4) and (5). According to Eq. (4), the interference term (i.e., the second term on the RHS

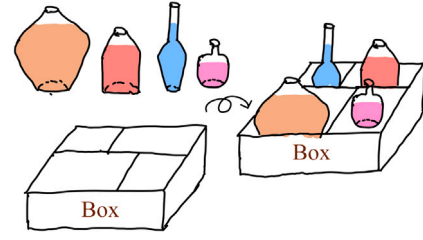


Fig. 5. Illustration of flexible virtual framework based lossless multi-user transmission (i.e., F³MAC).

of Eq. (4) under F³MAC is still 0. Moreover, compared to obtaining the gain of the k th eigenmode's of \mathbf{H}_k , i.e., $\lambda_k^{(k)}$, in Eq. (5), employing $\mathbf{w}_k = \mathbf{l}_{Fk}^{(1)}$ can yield the principal eigenmode's gain of \mathbf{H}_k , i.e., $\lambda_k^{(1)}$.

Similarly to the discussions about Eqs. (6)–(8) and (10) in Section 4.2, each Tx dynamically re-constructs \mathbf{R}_F and \mathbf{L}_F , and designs its precoding vector according to the re-constructed matrices. Rx adopts filter matrix $\mathbf{W} = [\mathbf{u}_{F1}^{(1)} \mathbf{u}_{F2}^{(1)} \cdots \mathbf{u}_{FK}^{(1)}] = [\mathbf{u}_F^{(1)} \mathbf{u}_F^{(2)} \cdots \mathbf{u}_F^{(K)}]$ to process the received mixed signal, so that F³MAC can realize multiple concurrent transmissions without interference in the virtual framework \mathbf{H}_F , whose CQI is replaced by the principal eigenmodes' gains of multiple users' channels.

Fig. 5 illustrates the lossless multi-user signal transmission based on the flexible virtual framework. As the figure shows, we divide the box into multiple grids that can adapt to different shapes and sizes of the beverage bottles. So, all beverages can keep their own characteristics, i.e., shapes and volumes, during packing and transportation (i.e., no transmission quality loss occurs).

From the above discussions, we can see that both F²MAC and F³MAC can guarantee orthogonality of multi-user transmissions with the virtual framework. The main difference is that in F³MAC each user first re-constructs the virtual framework, and then computes his/her precoder. As a result, F³MAC can not only eliminate CCI, but also preserve the principal eigenmode's gain of each user's channel, thus realizing high-fidelity lossless signal processing. Compared to F²MAC, F³MAC can yield higher system SE.

Table 1 compares some multi-user signal processing methods, including ZF based MAC (ZF-MAC), F²MAC and F³MAC. With ZF-MAC [23,24], users are at first sorted in descending order according to their principal eigenmodes' gains; next, the first column of the right singular matrix of each user's communication channel is selected as the initial precoding vector; then, orthogonal projection is applied to the initial precoders so that each adjusted precoder can be orthogonal to the subspace formed by the spatial features of other users' transmissions. With such ZF-based precoders, CCI can be mitigated. However, spatial features of users' signals are adjusted and no longer matches their channels, and thus loss of the transmission gain yields. Compared to the lossy ZF-MAC's adjusting signal's spatial feature and transmission quality simultaneously, F²MAC and F³MAC separately adjust the above two attributes of the users' transmissions so that multi-user transmissions are packed into a virtual point-to-point framework. That is, multi-user communication is equivalent to K independent interference-free p2pMIMO transmissions. According to F²MAC, the spatial features of users' signals are determined by the virtual framework; only one user (indexed with $k = l$ where l is arbitrarily chosen from set $\{1, 2, \dots, K\}$; note, however, in the previous discussion we take $k = 1$ for simplicity) can preserve the principal eigenmode's gain of his/her channel while the other users (indexed with $k \neq l$) can only obtain their secondary eigenmodes' gains. As for F³MAC, all users can obtain the principal eigenmodes' gains of their communication channels owing to the local re-construction of the framework.

Table 1
Comparison of various multi-user signal processing methods.

Method	Whether CQI and CDI are bound together	Initial gain of user's transmission	Transmit precoder design	Receive filter design
ZF-MAC [23,24]	Yes	Principal eigenmode's gain	\mathbf{p}_k is selected from the right-singular matrix of \mathbf{H}_k and adjusted in terms of the other users' transmissions	\mathbf{w}_k is selected to match Tx_k 's transmission in terms of MF
F ² MAC	No	Principal (indexed with $k = l$) and secondary (indexed with $k \neq l$) eigenmode's gain	$\mathbf{p}_k = \mathbf{A}_k \mathbf{r}_{Fk}^{(k)}$, $\mathbf{A}_k = \mathbf{H}_k^{-1} \mathbf{L}_F \mathbf{D}_k \mathbf{R}_F^H$	$\mathbf{w}_k = \mathbf{1}_F^{(k)}$
F ³ MAC	No	Principal eigenmode's gain	$\mathbf{p}_k = \mathbf{A}_k \mathbf{r}_{Fk}^{(1)}$, $\mathbf{A}_k = \mathbf{H}_k^{-1} \mathbf{L}_{Fk} \mathbf{D}_k \mathbf{R}_{Fk}^H$, $\mathbf{R}_{Fk} = \mathbf{R}_F \mathbf{E}(1, k)$	$\mathbf{w}_k = \mathbf{1}_F^{(1)}$, $\mathbf{L}_{Fk} = \mathbf{L}_F \mathbf{E}(1, k)$

4.4. Discussion about power overhead and eigenmode matching schemes for F²MAC and F³MAC

From the design of F²MAC and F³MAC, we can see that although these methods can realize lossless multi-user communication, their precoders are no longer unit vectors. That means both methods need to consume some transmit power to compensate for users' transmission gains. However, it is worth noting that although F²MAC and F³MAC incur power overhead, their compensation for multi-user transmission gains still has practical significance. On one hand, in traditional signal processing based MACs [25], each Tx employs precoding to adjust the spatial feature of its transmitted signal, and the common Rx designs filter matrix correspondingly to recover multiple desired data from the received mixed signal. The essence of such schemes is realizing concurrent multi-user transmissions at the cost of some loss of Tx's transmission rate. In other words, the desired data rate (or channel gain) of the Tx who sends to the Rx exclusively (i.e., employing point-to-point (p2p) transmission) is higher than that of the same Tx's transmission when the Tx coexists with the others. The difference of the above transmission rates in two situations depends not only on the quality of the channel between the Tx and Rx, but also the scheduling priority of the Tx and the number of Txs in the system [26]. Therefore, when a Tx with high single-user data rate participates in multi-user communication, its actual rate after comprising with other Txs may be degraded, hence hindering the Tx to take part in multi-user transmission. F²MAC and F³MAC can avoid such deficiency as all Txs' transmission gains are compensated based on their own channels. On the other hand, in practical mobile communication systems, in order to avoid the adjacent channel interference and near-far effect, both the BS and MS can realize automatic transmit power control to ensure that the signal power levels from various Txs to the Rx are approximately the same [27,28]. This method can provide technical basis for the implementation of F²MAC and F³MAC. To summarize, the proposed virtual framework based MAC methods are suitable for multi-user transmissions where the Txs have sufficient power supply, wide dynamic range of transmit power, and high demand for the transmission performance.

In what follows, we will analyze the power cost of F²MAC and F³MAC. We use \mathbf{p}_k to denote the precoding vector of Tx_k , then Tx_k 's power cost (normalized by P_T) can be represented by $\|\mathbf{p}_k\|^2$. As for F²MAC, the spatial correlation between the i th eigenmode of Tx_k 's channel \mathbf{H}_k and the j th eigenmode of the virtual framework \mathbf{H}_F , denoted by ρ_k^{ij} , affects Tx_k 's power cost (i.e., $\|\mathbf{p}_k\|^2$) for transmission gain compensation. Specifically, the larger ρ_k^{ij} , the less transmission gain loss is incurred while loading Tx_k 's transmission in the i th eigenmode of \mathbf{H}_k into the j th eigenmode of \mathbf{H}_F , and hence a reduced $\|\mathbf{p}_k\|^2$ is yielded. Similarly, under F³MAC, the spatial correlation between the principal eigenmode (indexed with $i = 1$) of Tx_k 's channel \mathbf{H}_k and the

j th eigenmode of \mathbf{H}_F , represented by ρ_k^{1j} , influences Tx_k 's $\|\mathbf{p}_k\|^2$. The higher ρ_k^{1j} , the less transmission gain loss is incurred while adjusting the data transmission in the principal eigenmode of \mathbf{H}_k into the j th eigenmode of \mathbf{H}_F , hence smaller $\|\mathbf{p}_k\|^2$ results.

Since Tx_k 's power overhead under F²MAC and F³MAC depends on $\lambda_k^{(i)}$ and ρ_k^{ij} , and $\lambda_k^{(1)}$ and ρ_k^{1j} , respectively, randomly matching \mathbf{H}_k 's eigenmode with \mathbf{H}_F 's may yield Tx_k adjusting its transmission to a less correlated \mathbf{H}_F 's eigenmode, hence incurring high power compensation cost. Then, in practice, in order to reduce the power cost for transmission gain compensation, we can match Tx 's eigenmode with \mathbf{H}_F 's based on their spatial correlation, i.e., packing user's transmission into \mathbf{H}_F 's eigenmode with as high correlation as possible.

Next, we will present the realization of F²MAC and F³MAC employing *Correlation-based Eigenmode Matching* (CEM) in Algorithms 1 and 2, respectively. Before delving into details of F²MAC and F³MAC with CEM, we first define sets Ω_1 and Ω_2 to represent the indices of unmatched eigenmodes of \mathbf{H}_F and the indices of Txs whose transmissions have not completed eigenmode matching. According to the assumptions given in the system model section, we have $N_T = N_R = K$; then we can initialize both sets as $\Omega_1 = \Omega_2 = \{1, \dots, K\}$. Moreover, we define the maximum value of the correlation between the user channel's and \mathbf{H}_F 's eigenmodes as ρ_{max} . The index of Tx who has completed eigenmode matching is denoted by k_* . The indices of Tx_{k_*} 's and \mathbf{H}_F 's eigenmodes which have completed matching are represented by i_* and j_* , respectively. ρ_{max} , k_* , i_* and j_* are initialized to be 0.

Algorithm 1 F²MAC with CEM

```

1: while  $\Omega_1 \neq \emptyset$  and  $\Omega_2 \neq \emptyset$  do
2:   for  $i = 1$  to  $K$  step 1 do
3:     for  $j \in \Omega_1$  do
4:       for  $k \in \Omega_2$  do
5:         Calculate  $\rho_k^{ij} = \|[\mathbf{u}_k^{(i)}]^H \mathbf{u}_F^{(j)}\|^2$ .
6:         if  $\rho_k^{ij} > \rho_{max}$  then
7:            $i_* \leftarrow i$ ,  $j_* \leftarrow j$ ,  $k_* \leftarrow k$ ,  $\rho_{max} \leftarrow \rho_k^{ij}$ .
8:         end if
9:       end for
10:     end for
11:   end for
12:   Match the  $i_*^{th}$  eigenmode of  $\mathbf{H}_{k_*}$  with the  $j_*^{th}$  eigenmode of  $\mathbf{H}_F$  with F2MAC;
13:    $\Omega_1 \leftarrow \Omega_1 - \{j_*\}$ ,  $\Omega_2 \leftarrow \Omega_2 - \{k_*\}$ ,  $\rho_{max} \leftarrow 0$ .
14: end while

```

In Algorithms 1 and 2, we select the channel matrix \mathbf{H}_k where $k \in \{1, \dots, K\}$ with the largest principal eigenmode's gain as \mathbf{H}_F , namely the *maximum gain framework*. This is because: (1) When CEM is employed, upon adopting the maximum gain framework, both F²MAC and F³MAC can pack the transmission of the Tx with the largest principal gain

Algorithm 2 F³MAC with CEM

```

1: while  $\Omega_1 \neq \emptyset$  and  $\Omega_2 \neq \emptyset$  do
2:   for  $j \in \Omega_1$  do
3:     for  $k \in \Omega_2$  do
4:       Calculate  $\rho_k^{1j} = \|\mathbf{u}_k^{(1)H} \mathbf{u}_F^{(j)}\|^2$ .
5:       if  $\rho_k^{1j} > \rho_{max}$  then
6:          $j_* \leftarrow j, k_* \leftarrow k, \rho_{max} \leftarrow \rho_k^{1j}$ .
7:       end if
8:     end for
9:   end for
10:  Match the principal eigenmode of  $\mathbf{H}_{k_*}$  with the  $j_*^{th}$  eigenmode of  $\mathbf{H}_F$  with F3MAC;
11:   $\Omega_1 \leftarrow \Omega_1 - \{j_*\}, \Omega_2 \leftarrow \Omega_2 - \{k_*\}, \rho_{max} \leftarrow 0$ .
12: end while

```

into \mathbf{H}_F 's principal eigenmode, hence yielding high transmission gain without power compensation. As a comparison, with *random gain framework*, i.e., \mathbf{H}_F is randomly selected from all users' channels, although the Tx whose channel has been selected as \mathbf{H}_F can preserve its principal eigenmode's gain without power cost, when its gain is small, only low data rate can be yielded. (2) When *Random Eigenmode Matching* (REM) is employed, if we employ the maximum gain framework, the Tx's transmission in the maximum-gain principal eigenmode can be packed into the principal eigenmode of \mathbf{H}_F (i.e., outputting high data rate without extra power cost) with non-zero probability. As a comparison, when we adopt random gain framework, the user channel with non-maximum principal eigenmode's gain may be selected as \mathbf{H}_F . In such a case, although REM has chance to pack the transmission of the Tx with the largest principal eigenmode's gain into \mathbf{H}_F 's principal eigenmode, and moreover, with both F²MAC and F³MAC, such maximum principal eigenmode's gain can be preserved, transmit power overhead for gain compensation is incurred. Based on the above discussion, in order to achieve good SE performance with low power consumption, one should employ the Tx's channel with the largest principal eigenmode's gain as \mathbf{H}_F .

Algorithm 3 Hybrid F^{2&3}MAC with CEM

```

1: while  $\Omega_1 \neq \emptyset$  and  $\Omega_2 \neq \emptyset$  do
2:   Execute lines 2 to 9 in Algorithm 2.
3:   if  $\rho_{max} \geq \rho_{th}$  then
4:     Match the principal eigenmode of  $\mathbf{H}_{k_*}$  with the  $j_*^{th}$  eigenmode of  $\mathbf{H}_F$  with F3MAC;
5:      $\Omega_1 \leftarrow \Omega_1 - \{j_*\}, \Omega_2 \leftarrow \Omega_2 - \{k_*\}, \rho_{max} \leftarrow 0$ .
6:   else
7:     break.
8:   end if
9: end while
10: Execute lines 1 to 14 in Algorithm 1.

```

Note that Tx_k's transmission gain obtained with F³MAC is $\lambda_k^{(1)}$, whereas that obtained under F²MAC is $\lambda_k^{(i)}$ ($i \geq 1$). Then, given $i > 1$, SE of Tx_k under F²MAC is inferior to that with F³MAC; moreover, since $\lambda_k^{(1)} > \lambda_k^{(i)}$, F²MAC's power overhead is less than F³MAC's provided with $\rho_k^{1j} \geq \rho_k^{ij}$. So, in order to balance the power cost and SE performance, we can adaptively use F²MAC and F³MAC, namely *Hybrid F^{2&3}MAC*. In Hybrid F^{2&3}MAC, we employ a correlation threshold ρ_{th} for the adaptation of F²MAC and F³MAC. When $\rho_k^{1j} \geq \rho_{th}$, the power cost for gain compensation is relatively low, so we adopt F³MAC to pack the transmission in Tx_k's principal eigenmode into \mathbf{H}_F 's j th eigenmode. Otherwise, when $\rho_k^{1j} < \rho_{th}$, F³MAC incurs more power overhead for transmission gain compensation, then F²MAC becomes preferable. We present Hybrid F^{2&3}MAC with CEM as Algorithm 3.

According to the above descriptions, we can see that F²MAC and F³MAC with CEM are special cases of Hybrid F^{2&3}MAC with CEM.

Table 2

The complexity of main operations.

Operation	FLOP counts
$\mathbf{A}_1 + \mathbf{A}_1$	$2mn$
$\mathbf{A}_1 \mathbf{A}_2$	$6mnp + 2mp(n-1)$
\mathbf{A}_2^{-1}	$6m^3 + 2m(m-1)^2$
SVD(\mathbf{A}_1)	$24m^2n + 48mm^2 + 54n^3$
$\ \mathbf{A}_1\ _F$	$4mn$ [30]

Specifically, F²MAC with CEM can be regarded as Hybrid F^{2&3}MAC with CEM under $\rho_{th} = 1$, while F³MAC with CEM is equivalent to Hybrid F^{2&3}MAC with CEM under $\rho_{th} = 0$, respectively. The analysis is as follows. Since we adopt the maximum gain framework, the spatial correlation between the maximum principal eigenmode and \mathbf{H}_F 's principal eigenmode is 1; therefore, both F²MAC and F³MAC with CEM will match the above two principal eigenmodes. As for the other Tx's eigenmodes, their correlation with \mathbf{H}_F 's eigenmodes is less than 1. So, given $\rho_{th} = 1$, F²MAC with CEM is adopted to adjust these Tx's transmissions into \mathbf{H}_F 's eigenmodes. That is, under $\rho_{th} = 1$, Hybrid F^{2&3}MAC with CEM is equivalent to F²MAC with CEM. When $\rho_{th} = 0$, since the spatial correlation between each Tx's principal eigenmode and \mathbf{H}_F 's eigenmode is greater than 0, all Tx's principal eigenmodes will be matched with \mathbf{H}_F 's following F³MAC with CEM. That is, when $\rho_{th} = 0$, Hybrid F^{2&3}MAC with CEM becomes F³MAC with CEM.

In practice, the Tx's can determine the correlation threshold ρ_{th} based on their transmit power, channel conditions, and SE requirements. Besides the above adaption, there exist other criteria for adaption in practical use. For example, defining the transmission rate of Tx_k as r_k which can be calculated according to Shannon's theory, one can employ a coefficient $\sum_{k=1}^K r_k / \sum_{k=1}^K \|\mathbf{p}_k\|^2$ indicating energy efficiency for F²MAC/F³MAC adaptation. Specifically, if $\sum_{k=1}^K r_k / \sum_{k=1}^K \|\mathbf{p}_k\|^2$ under F²MAC is greater than that under F³MAC, F²MAC is adopted; otherwise, if F³MAC outputs a larger $\sum_{k=1}^K r_k / \sum_{k=1}^K \|\mathbf{p}_k\|^2$, F³MAC should be employed. Since the above adaptation criterion incurs extra computational complexity, we do not elaborate on it in this paper. Instead, we employ ρ_{th} -based adaption as discussed in this subsection for simplicity.

4.5. Analysis of computational complexity

In this subsection, we will analyze the computational complexity of the proposed schemes. According to [29], the complexity is quantified in the number of real floating-point operations (FLOPs). A real addition, multiplication, or division is counted as one FLOP. A complex addition and multiplication have two FLOPs and six FLOPs, respectively. First, we give the complexity of main operations in Table 2, where $\mathbf{A}_1 \in \mathbb{C}^{m \times p}$, $\mathbf{A}_2 \in \mathbb{C}^{m \times p}$ and $\mathbf{A}_3 \in \mathbb{C}^{m \times m}$.

Based on the parameter settings suggested in Section 4, we will give the complexity analysis under $N_T = N_R = N$, and the number of users (Tx's) K satisfies $K \leq N$. For F²MAC with REM, the common Rx first randomly selects a framed matrix $\mathbf{H}_F \in \mathbb{C}^{N_R \times N_T}$ from K channel matrices related to the K Tx's and applies SVD to it to have $\mathbf{H}_F = \mathbf{U}_F \mathbf{D}_F \mathbf{V}_F^H$, and then broadcasts the results to all Tx's. This operation takes $126N^3$ FLOPs. Next, each Tx, say Tx_k where $k \in \{1, 2, \dots, K\}$, applies SVD to its communication channel \mathbf{H}_k to get $\mathbf{H}_k = \mathbf{U}_k \mathbf{D}_k \mathbf{V}_k^H$. This operation takes $126KN^3$ FLOPs. Then, Tx_k calculates its precoding vector $\mathbf{p}_k = \mathbf{H}_k^{-1} \mathbf{U}_F \mathbf{D}_k \mathbf{V}_F^H \mathbf{v}_F^{(k)}$ which contains an inversion operation and four matrix/vector multiplications. Thus, obtaining \mathbf{p}_k takes $8KN^3 + 28KN^2 - 6KN$ FLOPs. Since the filtering vector is directly obtained from the SVD of \mathbf{H}_F , no extra computation complexity is incurred. Based on the above analysis, the FLOP count of F²MAC with REM is $134KN^3 + 126N^3 + 28KN^2 - 6KN$.

As F²MAC's counterpart, F³MAC with REM incurs the reconstruction of K Tx's left and right framed matrices, i.e., calculating $\mathbf{U}_{Fk} = \mathbf{U}_F \mathbf{E}(1, k)$ and $\mathbf{V}_{Fk} = \mathbf{V}_F \mathbf{E}(1, k)$, respectively. This operation takes $16KN^3 - 4KN^2$ FLOPs. Therefore, the FLOP count of F³MAC with REM is $150KN^3 + 126N^3 + 24KN^2 - 6KN$.

As for F^2 MAC with CEM, its complexity can be calculated according to Algorithm 1. As the algorithm presents, each loop includes a complex vector calculation $\rho^{ij} = \|\mathbf{u}_k^{(i)H} \mathbf{u}_k^{(j)}\|^2$, and the number of loops is $N^2 + (N-1)^2 + \dots + (N-K+1)^2 = (6KN^2 - 6K^2N + 2K^3 + 6KN - 3K^2 + K)/6$. Since each calculation of ρ^{ij} takes $8N + 3$ FLOPs, the total FLOP count of Algorithm 1 is $(48KN^3 - 48K^2N^2 + 16K^3N + 66KN^2 - 42K^2N + 6K^3 + 26KN - 9K^2 + 3K)/6$. Recall that SVD in the use of F^2 MAC yields $134KN^3 + 126N^3 + 28KN^2 - 6KN$ FLOPs, we can get the FLOP count of F^2 MAC with CEM as $142KN^3 - 8K^2N^2 + 126N^3 + 39KN^2 - 7K^2N + K^3 + (16K^3N - 10KN^2 + 3K)/6$.

Similarly, according to Algorithm 2, we can get the computational complexity of F^3 MAC with CEM. In Algorithm 2, the number of loops is $N + (N-1) + \dots + (N-K+1) = (2KN - K^2 + K)/2$, each loop yields $8N + 3$ FLOPs, so the FLOP count of the algorithm is $(16KN^2 - 8K^2N + 14KN - 3K^2 + 3K)/2$. In addition, SVD in the use of F^3 MAC yields $150KN^3 + 126N^3 + 24KN^2 - 6KN$ FLOPs. Therefore, the total FLOP count of F^3 MAC with CEM is $150KN^3 + 126N^3 + 32KN^2 - 4K^2N + KN - 1.5K^2 + 1.5K$.

Under Hybrid $F^{2\&3}$ MAC with CEM, we can analyze its computational complexity according to Algorithm 3. As can be seen from Algorithm 3, Algorithm 2 is executed first, incurring $(2KN - K^2 + K)/2$ loops (each loop's complexity is $8N + 3$ FLOPs). Then, users satisfying $\rho_{max} < \rho_{th}$ execute Algorithm 1. Note that the number of loops in Algorithm 3 depends on the value of ρ_{th} . We define the number of users executing Algorithm 1 as $\mathcal{F}(K, \rho_{th})$ which is a function of K and ρ_{th} . However, determining $\mathcal{F}(K, \rho_{th})$ is difficult. Therefore, we analyze the upper and lower bounds of the computational complexity of Hybrid $F^{2\&3}$ MAC with CEM, i.e., F^3 MAC with CEM under $\rho_{th} = 0$ and F^2 MAC with CEM under $\rho_{th} = 1$, respectively. Specifically, we can get the upper bound ($\rho_{th} = 0$) of Hybrid $F^{2\&3}$ MAC's FLOP count as $150KN^3 + 126N^3 + 32KN^2 - 4K^2N + KN - 1.5K^2 + 1.5K$, and the lower bound ($\rho_{th} = 1$) as $142KN^3 - 8K^2N^2 + 126N^3 + 47KN^2 - 11K^2N + K^3 - 3K^2 + 2K + (16K^3N + 32KN)/6$ which is obtained by adding the FLOP counts of F^2 MAC with CEM to that of Algorithm 2. Therefore, the complexity of Hybrid $F^{2\&3}$ MAC with CEM lies between the above lower and upper bounds.

Based on the above discussion, F^3 MAC incurs the highest complexity, then comes Hybrid $F^{2\&3}$ MAC, and F^2 MAC ranks the third. However, it should be noticed that the order of the complexity of the three methods is identical, i.e., $\mathcal{O}(KN^3)$.

5. Evaluation

We use MATLAB simulation to evaluate the performance of the proposed MAC mechanisms. We set $N_T = N_R = K$ where $N_T, N_R, K \in \{2, 4\}$ and adopt maximum gain framework. Each Tx sends a single data stream with power P_T to the common Rx. We define the transmit power of Tx normalized by noise power σ_n^2 as $\eta = 10 \lg(P_T/\sigma_n^2)$, and set $\eta \in [-10, 20]$ dB in the simulation.

Besides the proposed F^2 MAC and F^3 MAC with CEM and REM, we also simulate MF, ZF reception, p2pMIMO and ZF-MAC [23,24] for comparison. With MF, each Tx employs SVD-based precoding in terms of its channel and adopts the principal eigenmode to transmit signals to Rx. Rx calculates K filter vectors, each of which matches a desired signal, then K signal components can be detected separately. The SINR of the k th desired signal under MF can be calculated as $\gamma_k = \frac{P_T \|\mathbf{w}_k^H \mathbf{H}_k \mathbf{p}_k\|^2}{P_T \sum_{i=1, i \neq k}^K \|\mathbf{w}_i^H \mathbf{H}_i \mathbf{p}_i\|^2 + \sigma_n^2}$ where $\mathbf{w}_k = \frac{\mathbf{H}_k \mathbf{p}_k}{\|\mathbf{H}_k \mathbf{p}_k\|}$ denotes the matched filter vector for data x_k . Under ZF reception, each Tx employs SVD based precoding in terms of its channel w.r.t. the Rx, and adopts the principal eigenmode to transmit to Rx. In decoding the k th signal, Rx treats the other $K-1$ unintended signal components as interferences. By selecting a filter vector located in the null space of the interferences to post-process the mixed signal, desired data without interference can be estimated. However, such signal processing incurs loss of the desired signal's power. As for ZF-MAC, users are at first sorted in

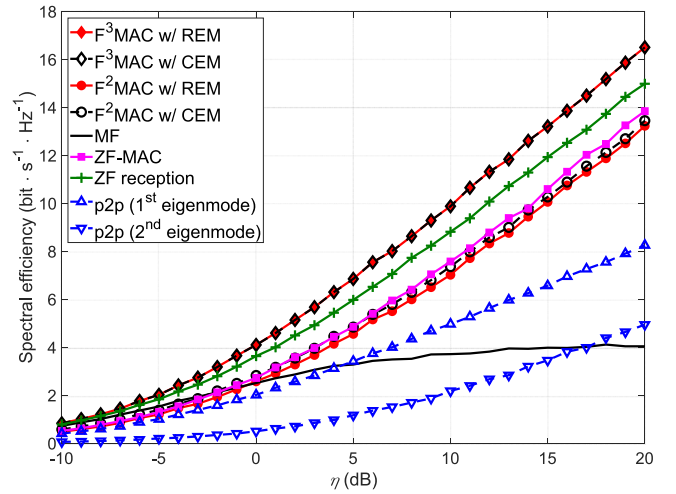


Fig. 6. System SE of various methods under $N_T = N_R = K = 2$ and different η s.

descending order according to their principal eigenmodes' gains; next, each user selects the first column of the right singular matrix of his/her communication channel as the initial precoding vector; then, the first user (indexed with $k = 1$) adopts his/her initial precoder as the final precoding vector, while the k th ($k > 1$) user projects his/her initial precoder to the subspace orthogonal to the one formed by the previous $k-1$ transmissions, so as to obtain his/her precoding vector. At the Rx side, filter vector for each Tx's data is determined according to the MF reception. Under ZF-MAC, only one user's transmission is lossless, whereas for the remaining $K-1$ users that are in descending order, loss of a user's transmission quality becomes severer as his/her index increases. In what follows, we will show 4 simulation figures. The first two figures are used to demonstrate the advantages of the proposed methods over existing MAC methods. From these two figures, we can also find that F^3 MAC outperforms F^2 MAC in system SE. Since such an SE improvement is obtained by consuming more transmit power, we then use Figs. 8 and 9 to illustrate the tradeoff between system SE and transmit power overhead.

Fig. 6 plots the system SE of various schemes under $N_T = N_R = K = 2$. As the figure shows, the averaged system SE of all mechanisms grows with the increase of η . F^3 MAC under REM and CEM achieves identical and the highest SE. This is because F^3 MAC can preserve the principal eigenmode's gain of each user; and eigenmode matching method does not affect F^3 MAC's SE, i.e., the compensated system SE only depends on users' communication channels. SE of ZF reception ranks the second, which is larger than that of F^2 MAC. This is because under ZF reception, each Tx employs its principal eigenmode for data transmission, while after filtering at the Rx, the loss of transmission gain compared to the principal eigenmode's gain is yielded. As a comparison, with F^2 MAC, only one user can preserve his/her principal eigenmode's gain, whereas the other $K-1$ users can only obtain their secondary eigenmodes' gains, so that SE of F^2 MAC is lower than that of ZF reception. Moreover, system SE of F^2 MAC with CEM slightly exceeds that of F^2 MAC with REM. This is because CEM can ensure the user with the largest principal eigenmode's gain to adjust its transmission into \mathbf{H}_F 's principal eigenmode, while REM may select the user with small principal eigenmode's gain to match \mathbf{H}_F 's principal eigenmode which incurs some SE loss compared to CEM. Given a large η (e.g., $\eta > 0$ dB), the SE of ZF-MAC is inferior to that of ZF reception, then F^2 MAC, and MF yields the lowest SE. Under a low η (e.g., $\eta < 0$ dB), MF's SE is close to F^3 MAC's and ZF reception's, and outperforms ZF-MAC's and F^2 MAC's. This is analyzed as follows. When η is low, noise dominates the system SE, and hence the reception quality (i.e., SINR or SNR) of each user is mainly determined by the effective desired signal's power and strength

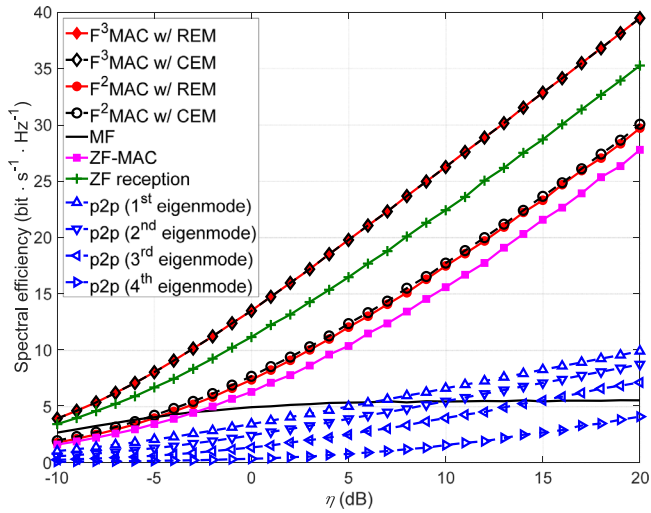


Fig. 7. System SE of various methods under $N_T = N_R = K = 4$ and different η .

of noise. Although ZF reception and ZF-MAC can mitigate interference, the SE improvement brought by interference management is close to (e.g., ZF reception) or even less than (e.g., ZF-MAC) the SE loss incurred by desired transmission's power reduction in signal processing. As η grows larger, interference becomes dominant for system SE. Since F^3 MAC, F^2 MAC, ZF reception and ZF-MAC can realize interference-free transmission, their SE grows with an increase of η . As for MF, although larger η indicates that the strength of users' signals perceived by Rx increases, since MF leaves CCI un-managed, disturbances at Rx become severer. Therefore, the system SE of MF saturates at a high η , and is lower than that of the other IM-based methods. Moreover, it is worth noting that under $N_T = N_R = K = 2$, F^2 MAC's system SE is the sum of the SEs of p2pMIMO employing the principal and secondary eigenmodes, respectively; while SE of F^3 MAC is 2x that of p2pMIMO adopting the principal eigenmode. These results are in consistent with our theoretical analysis. As a conclusion, under $N_T = N_R = K = 2$, F^3 MAC with REM and CEM can output the highest SE, ZF ranks the second, then come F^2 MAC with CEM and REM, respectively. Moreover, the proposed methods can outperform MF and ZF-MAC.

Fig. 7 plots the system SE of various methods under $N_T = N_R = K = 4$. One can see that given the same η , system SE of F^2 MAC, F^3 MAC, ZF-MAC and ZF reception outperforms that in Fig. 6. Such an improvement is made by increasing the numbers of users and antennas at both Tx- and Rx-sides. Since MF cannot eliminate CCI, its system SE is not obviously improved over that in Fig. 6. As Fig. 7 shows, F^2 MAC outperforms ZF-MAC in system SE, because although both methods can mitigate CCI, F^2 MAC determines signals' precoding vectors based on the virtual framework without considering the spatial features of other users' transmissions, thus achieving no transmission gain loss. On the other hand, for ZF-MAC, Tx employs precoding based on orthogonal projection to avoid interference to other users' transmissions, hence incurring a severer transmission gain loss as the number of users grows. Therefore, the system SE of ZF-MAC is inferior to that of F^2 MAC. Moreover, under $N_T = N_R = K = 4$, F^2 MAC's system SE is the sum of the SEs of p2pMIMO employing four eigenmodes, while SE of F^3 MAC is 4x that of p2pMIMO adopting the principal eigenmode. From the above discussion we can conclude that under $N_T = N_R = K = 4$, F^3 MAC can output the highest SE, ZF ranks the second, then come F^2 MAC. The proposed methods excel MF and ZF-MAC in system SE.

Next, we simulate the power overhead and system SE of the proposed methods. We set $\rho_{th} \in \{0.25, 0.5, 0.75\}$. Fig. 8 plots the system SE of various methods under $N_T = N_R = K = 4$. As the figure shows, the average system SE of all mechanisms grows with the increase of η . With F^3 MAC, the system SE obtained under REM and CEM is

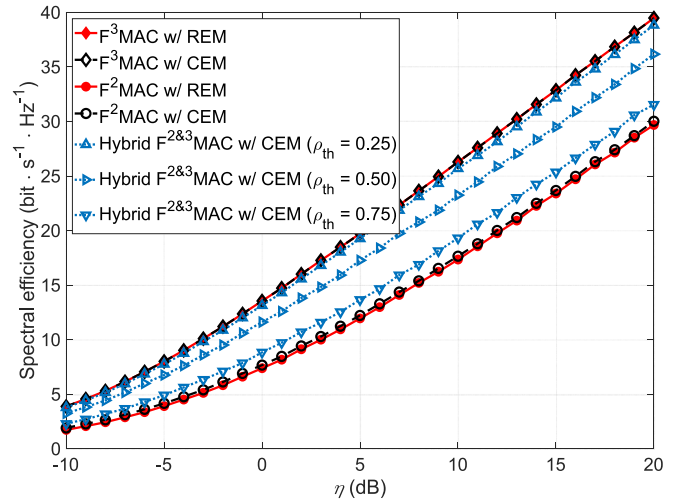


Fig. 8. Comparison of Hybrid $F^{2\&3}$ MAC and exclusive F^2/F^3 MAC under $N_T = N_R = K = 4$ and different η .

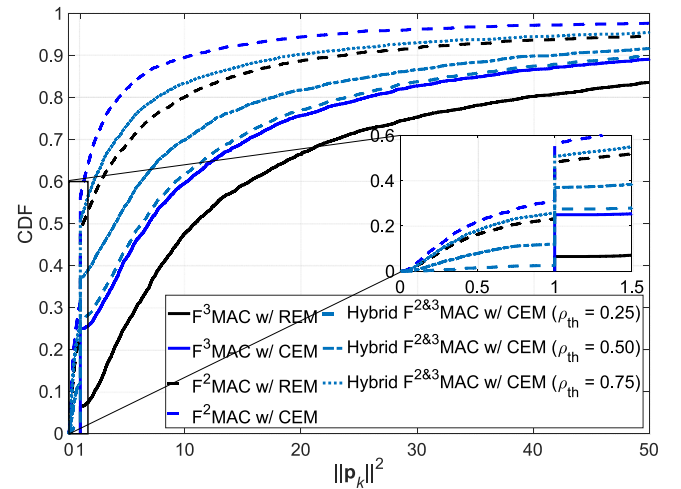


Fig. 9. CDF of $\|\mathbf{p}_k\|^2$ under $N_T = N_R = K = 4$.

identical and superior to that under the other methods. Since F^2 MAC can only let one Tx transmit with its principal eigenmode's gain, while the others preserve their secondary eigenmodes' gains which yields relatively small SE, it outputs the lowest SE. System SE of F^2 MAC with CEM slightly excels that of F^2 MAC with REM. The analysis can be found in the discussions about Fig. 6. System SE of Hybrid $F^{2\&3}$ MAC with CEM decreases as ρ_{th} grows, and approaches F^3 MAC and F^2 MAC with CEM under $\rho_{th} = 0.25$ and $\rho_{th} = 0.75$, respectively. This is because with the increase of ρ_{th} , the number of users whose transmission's correlation with \mathbf{H}_F 's eigenmode can reach ρ_{th} decreases, so that fewer users pre-process their signals with F^3 MAC and more users with F^2 MAC, thus yielding a decrease of system SE. As a conclusion, F^3 MAC outperforms F^2 MAC in system SE. SE of Hybrid $F^{2\&3}$ MAC lies between that of F^3 MAC and F^2 MAC. The smaller ρ_{th} is, the higher system SE Hybrid $F^{2\&3}$ MAC yields.

Fig. 9 plots the cumulative distribution function (CDF) of user's power overhead with various methods under $N_T = N_R = K = 4$. As the figure shows, the CDF curves of all methods are discontinuous at $\|\mathbf{p}_k\|^2 = 1$. To be specific, as $\|\mathbf{p}_k\|^2$ grows from 1_- to 1_+ the CDF curves of F^2 MAC with CEM/REM and Hybrid $F^{2\&3}$ MAC with CEM under different ρ_{th} s jump from various non-zero values to larger ones

at $\|\mathbf{p}_k\|^2 = 1$, the steps are approximately 0.25; as for F³MAC with CEM and REM, their CDF values under $\|\mathbf{p}_k\|^2 < 1$ are 0 and jump to about 0.25 and 0.0625, respectively, at $\|\mathbf{p}_k\|^2 = 1$. The analysis is as follows. As for those F²MAC-related methods, a Tx, say Tx_k, may load its transmission in one of its secondary eigenmodes, e.g., eigenmode i , into \mathbf{H}_F 's j th eigenmode. In the case of $i \neq j$, we let the Tx (i.e., Tx_k) preserve its j th eigenmode's gain in the simulation. Since there is probability that $i < j$, in such a case the preserved transmission gain is reduced from $\lambda_k^{(i)}$ to $\lambda_k^{(j)}$, then even the correlation between Tx_k's i th eigenmode and \mathbf{H}_F 's j th eigenmode is less than 1, $\|\mathbf{p}_k\|^2$ less than 1 may result, yielding CDF values of the F²MAC-related methods under $\|\mathbf{p}_k\|^2 < 1$ being non-zero. As a comparison, since all Txs preserve their principal eigenmodes' gains, they need to consume extra power while loading their transmissions into \mathbf{H}_F , so that under F³MAC with CEM and REM the probability that $\|\mathbf{p}_k\|^2 \geq 1$ is 1, yielding the CDF values of these methods under $\|\mathbf{p}_k\|^2 < 1$ being 0. As for the discontinuity of CDF curves of F²MAC-related methods and F³MAC with CEM at $\|\mathbf{p}_k\|^2 = 1$, since we adopt a Tx's channel as \mathbf{H}_F , the probability that one Tx's precoder satisfies $\|\mathbf{p}_k\|^2 = 1$ is $\frac{1}{K}$, yielding $Prob(\|\mathbf{p}_k\|^2 \leq 1) = Prob(\|\mathbf{p}_k\|^2 < 1) + Prob(\|\mathbf{p}_k\|^2 = 1) = Prob(\|\mathbf{p}_k\|^2 < 1) + \frac{1}{K}$. Note that we set $K = 4$ in the simulation, thus the variation of CDF values under F²MAC-related methods and F³MAC with CEM at $\|\mathbf{p}_k\|^2 = 1$ is approximately 0.25. As for F³MAC with REM, since a Tx's transmission is randomly adjusted into \mathbf{H}_F 's eigenmode, the probability that the Tx with the maximum principal eigenmode's gain (this Tx's communication channel is adopted as \mathbf{H}_F) loads its principal transmission into \mathbf{H}_F 's principal eigenmode is $\frac{1}{K^2}$. Then, under $K = 4$, we can get the variation of F³MAC with REM's CDF value at $\|\mathbf{p}_k\|^2 = 1$ is about 0.0625.

As Fig. 9 plots, the power cost of F²MAC is less than that of F³MAC. This is because for Tx_k, the preserved transmission gain under F²MAC is $\lambda_k^{(i)}$ ($i \geq 1$), whereas for F³MAC, the compensated gain is $\lambda_k^{(1)}$. Then, given $i > 1$, since $\lambda_k^{(1)} > \lambda_k^{(i)}$ holds, F²MAC's power cost is less than F³MAC's under $\rho_k^{ij} \geq \rho_k^{1j}$ where j is the index of \mathbf{H}_F 's eigenmode into which Tx_k's transmission in \mathbf{H}_k 's i th eigenmode is adjusted. Moreover, power cost of F²MAC and F³MAC with CEM is less than that with REM. This is because the latter does not take spatial correlation between Tx's and \mathbf{H}_F 's eigenmodes into account. Therefore, loading user's transmission into a less correlated \mathbf{H}_F 's eigenmode will incur severe transmission gain loss, hence requiring the Tx to spend more power for gain compensation. As for Hybrid F^{2&3}MAC with CEM, its power cost reduces with the increase of ρ_{th} . This is because as ρ_{th} grows, an increasing number of Txs will adopt F²MAC instead of F³MAC for signal processing; and as aforementioned, power cost of F²MAC is lower than that of F³MAC, so a decrease of power compensation cost results. We can conclude from Fig. 9 that the power cost of F²MAC is less than that of F³MAC. With an increase of ρ_{th} , the power overhead of Hybrid F^{2&3}MAC reduces and approaches that of F²MAC.

Based on Figs. 8 and 9, we can find that although F³MAC can output the highest system SE, it consumes more transmit power than F²MAC. That is, only using one of the proposed methods cannot adapt to the randomly varying wireless environment and meet the communication system's demand. By adopting a proper ρ_{th} in applying Hybrid F^{2&3}MAC, we can adaptively use F³MAC and F²MAC, hence balancing system SE and power overhead. Specifically, the larger ρ_{th} , the smaller Tx's power cost and system SE; and vice versa. In practice, we can flexibly select ρ_{th} according to various communication requirements, e.g., maximizing system SE, limiting total transmit power consumption, etc.

6. Conclusion

We have proposed a framed fidelity multi-user transmission MAC (F²MAC) based on a virtual framework to remedy the deficiencies of traditional MAC methods which incur users' transmission performance loss when managing CCI. By introducing a virtual framed-channel in

precoding and filter design, F²MAC can separate CQI from CDI in signal processing, thus avoiding the loss of transmission quality. Moreover, since with F²MAC only one user can preserve his/her principal eigenmode's gain while the others can only maintain their secondary eigenmodes, we have also developed an improved version of F²MAC, called F³MAC. By adjusting the virtual framework at each Tx, a user's transmission can be realized with the principal eigenmode's gain of his/her own channel so that the system SE of F²MAC can be improved further. We also analyze the power overhead of the proposed methods and present Hybrid F^{2&3}MAC to balance the system SE and power consumption. Our simulation results have shown the proposed MAC methods to significantly improve the SE of multi-user communication systems.

CRedit authorship contribution statement

Zhao Li: Conceptualization, Methodology, Writing – original draft, Writing – review & editing. **Bigui Zhang:** Software, Validation, Data curation, Writing – original draft, Formal analysis. **Chengyu Liu:** Formal analysis, Validation, Software. **Zhixian Chang:** Writing – original draft, Methodology. **Kang G. Shin:** Supervision, Writing – review & editing, Funding acquisition. **Zheng Yan:** Supervision, Writing – review & editing, Funding acquisition.

Declaration of competing interest

The authors declare that they have no known competing financial interests or personal relationships that could have appeared to influence the work reported in this paper.

Data availability

No data was used for the research described in the article.

Acknowledgments

This work was supported in part by the Natural Science Foundation of Shaanxi Province, China under Grant 2021JM-143; the National Natural Science Foundation of China under Grant 62072351; the Fundamental Research Funds for the Central Universities, China under Grant JB211502; the Project of Key Laboratory of Science and Technology on Communication Network, China under Grant 6142104200412; the U.S. National Science Foundation under Grant CNS-1646130; the Academy of Finland under Grant 308087, Grant 335262 and Grant 345072; ZheJiang Lab, China; the Shaanxi Innovation Team Project, China under Grant 2018TD-007; and the 111 Project, China under Grant B16037.

References

- [1] Y. Cai, Z. Qin, et al., Modulation and multiple access for 5G networks, *IEEE Commun. Surveys Tuts.* 20 (1) (2018) 629–646.
- [2] M. Agiwal, A. Roy, N. Saxena, Next generation 5G wireless networks: A comprehensive survey, *IEEE Commun. Surveys Tuts.* 18 (3) (2016) 1617–1655.
- [3] D. Zucchetto, A. Zanella, Multi-rate ALOHA protocols for machine-type communication, in: *Proc. IEEE Intl. Conf. on Computing Networking and Commun., ICNC*, 2018, pp. 524–530.
- [4] S. Sen, R. Roy Choudhury, S. Nelakuditi, CSMA/CN: Carrier sense multiple access with collision notification, *IEEE Trans. Netw.* 20 (2) (2012) 544–556.
- [5] A. Aijaz, A. Hamid Aghvami, On the use and optimization of PRMA based cognitive M2M communications, in: *Proc. IEEE Global Telecommun. Conf., GLOBECOM*, 2013, pp. 1265–1271.
- [6] M. Ganji, X. Zou, H. Jafarkhani, Exploiting time asynchrony in multi-user transmit beamforming, *IEEE Trans. Wireless Commun.* 19 (5) (2020) 3156–3169.
- [7] M.S. Gast, 802.11ac: A Survival Guide, O'Reilly Media, USA, 2013.
- [8] Further Advancements for E-UTRA, Physical Layer Aspects; Coordinated Multiple Point Transmission and Reception, document 3GPP TR 36.815, 2010.
- [9] R. Liu, Z. Li, L. Xiao, Proactive CCI evaluation and transmission gain based scheduling for MU-MIMO broadcast channel, in: *Proc. IEEE Intl. Conf. on Wireless Commun. & Signal Processing, WCSP*, 2013, pp. 1–6.

- [10] A. Benjebbour, Y. Saito, et al., Concept and practical considerations of Non-Orthogonal Multiple Access (NOMA) for future radio access, in: Proc. Intl. Symp. Intell. Signal Proc. Commun. Syst., ISPACS, 2013, pp. 770–774.
- [11] H. Nikopour, H. Baligh, Sparse code multiple access, in: Proc. IEEE Intl. Symp. Personal Indoor Mobile Radio Commun, PIMRC, 2013, pp. 332–336.
- [12] S. Chen, B. Ren, et al., Pattern division multiple access — A novel nonorthogonal multiple access for fifth-generation radio networks, *IEEE Trans. Veh. Technol.* 66 (4) (2017) 3185–3196.
- [13] Z. Ding, X. Lei, et al., A survey on Non-Orthogonal Multiple Access for 5G networks: Research challenges and future trends, *IEEE J. Sel. Areas Commun.* 35 (10) (2017) 2181–2195.
- [14] C. Pan, J. Geng, et al., Linear detection and precoding for physical network coding in two-way MIMO relay channels, in: Proc. IEEE Veh. Technol. Conf, VTC Fall, 2011, pp. 1–4.
- [15] D. Tse, P. Viswanath, *Fundamentals of Wireless Communication*, Cambridge, U.K, Cambridge University Press, 2005.
- [16] G. Kwon, N. Kim, H. Park, Millimeter wave SDMA with limited feedback: RF-only beamforming can outperform hybrid beamforming, *IEEE Trans. Veh. Technol.* 68 (2) (2019) 1534–1548.
- [17] C.M. Yetis, T. Gou, S.A. Jafar, et al., On feasibility of interference alignment in MIMO interference networks, *IEEE Trans. Signal Process.* 58 (9) (2010) 4771–4782.
- [18] Z. Li, Y. Liu, K.G. Shin, et al., Interference steering to manage interference in IoT, *IEEE Internet Things J.* 6 (6) (2019) 10458–10471.
- [19] Y. Saito, A. Benjebbour, et al., System-level performance evaluation of downlink Non-Orthogonal Multiple Access (NOMA), in: Proc. IEEE Intl. Symp. Personal Indoor Mobile Radio Commun, PIMRC, 2013, pp. 611–615.
- [20] M. Baghani, S. Parsaeefard, et al., Dynamic Non-Orthogonal Multiple Access and orthogonal multiple access in 5G wireless networks, *IEEE Trans. Commun.* 67 (9) (2019) 6360–6373.
- [21] T. Park, G. Lee, et al., Sum rate and reliability analysis for power-domain nonorthogonal multiple access (PD-NOMA), *IEEE Internet Things J.* 8 (12) (2021) 10160–10169.
- [22] D.H.N. Nguyen, H. Nguyen-Le, T. Le-Ngoc, Block-diagonalization precoding in a multiuser multicell MIMO system: Competition and coordination, *IEEE Trans. Wireless Commun.* 13 (2) (2014) 968–981.
- [23] E. Castañeda, A. Silva, A. Gameiro, M. Kountouris, An overview on resource allocation techniques for multi-user MIMO systems, *IEEE Commun. Surv. Tut.* 19 (1) (2017) 239–284.
- [24] X. Zhang, *Matrix Analysis and Applications*, Cambridge University Press, U.K, 2017.
- [25] M.A. Albreem, M. Juntti, S. Shahabuddin, Massive MIMO detection techniques: A survey, *IEEE Commun. Surveys Tuts.* 21 (4) (2019) 3109–3132.
- [26] H.J. Kushner, P.A. Whiting, Convergence of proportional-fair sharing algorithms under general conditions, *IEEE Trans. Wireless Commun.* 3 (4) (2004) 1250–1259.
- [27] V. Sharma, U. Mukherji, et al., Optimal energy management policies for energy harvesting sensor nodes, *IEEE Trans. Wireless Commun.* 9 (2008) 1326–1336.
- [28] O. Ozel, K. Tutuncuoglu, et al., Transmission with energy harvesting nodes in fading wireless channels: Optimal policies, *IEEE J. Sel. Areas Commun.* 29 (8) (2011) 1732–1743.
- [29] Z. Li, J. Chen, et al., Coordinated multi-point transmissions based on interference alignment and neutralization, *IEEE Trans. Wirel. Commun.* 18 (7) (2019) 3347–3365.
- [30] J.H. Lee, W. Choi, Interference alignment by opportunistic user selection in 3-user MIMO interference channels, in: Proc. IEEE Intl. Conf. Commun, ICC, 2011, pp. 1–5.



Zhao Li received the B.S. degree in telecommunications engineering and the M.S. and Ph.D. degrees in communication and information systems from Xidian University, Xi'an, China, in 2003, 2006, and 2010, respectively. He worked as a Visiting Scholar and then Research Scientist with the Real-Time Computing Laboratory, Department of Electrical Engineering and Computer Science, University of Michigan, from 2013 to 2015. He is currently an Associate Professor with the School of Cyber Engineering, Xidian University. He has published over 40 technical articles at premium international journals and conferences, such as IEEE INTERNET OF THINGS JOURNAL, IEEE TRANSACTIONS ON WIRELESS COMMUNICATIONS (TWC), IEEE INFOCOM, IEEE TRANSACTIONS ON VEHICULAR TECHNOLOGY (TVT), Computer Communications, and Wireless Networks. His research interests include wireless communication, 5G communication systems, resource allocation, interference management, the IoT, and physical layer security.



Bigui Zhang is currently a Master's student with the School of Cyber Engineering at Xidian University. Her research interests include wireless communication, resource allocation, medium access control, and interference management.



Chengyu Liu is currently a Master's student with the School of Cyber Engineering at Xidian University. His research interests include wireless communication, medium access control, and interference management.



Zhixian Chang received the B.S. degree in telecommunications engineering, and the MS degrees in communication and information systems from Xidian University, Xi'an, China, in 2003 and 2006, respectively. She is currently a Lecturer in the School of Communications and Information Engineering, Xi'an University of Posts & Telecommunications, Xi'an, China. She has published over 10 technical papers at premium international journals and conferences. Her research interests include wireless communication, 5G, resource allocation, network slicing, green radio network and software defined network.



Kang G. Shin received the B.S. degree in electronics engineering from Seoul National University, Seoul, South Korea, in 1970, and the M.S. and Ph.D. degrees in electrical engineering from Cornell University, Ithaca, NY, USA, in 1976 and 1978, respectively. He is currently the Kevin and Nancy O'Connor Professor of Computer Science and the Founding Director of the Real-Time Computing Laboratory, Department of Electrical Engineering and Computer Science, University of Michigan, Ann Arbor, MI, USA. At Michigan, he has supervised the completion of 82 PhDs and also chaired the Computer Science and Engineering Division for three years starting in 1991. From 1978 to 1982, he was on the faculty of the Rensselaer Polytechnic Institute, Troy, NY, USA. He has authored/coauthored more than 900 technical articles (more than 330 of which are published in archival journals) and more than 30 patents or invention disclosures. His current research interests include QoS-sensitive computing and networks as well as on embedded real-time and cyber-physical systems. He is also a fellow of ACM. He received numerous institutional awards and best paper awards.



Zheng Yan received the B.Eng. degree in electrical engineering and the M.Eng. degree in computer science and engineering from Xi'an Jiaotong University, Xi'an, China, in 1994 and 1997, respectively, the M.Eng. degree in information security from the National University of Singapore, Singapore, in 2000, and the Lic.Sc. degree and the D.Sc. (Tech.) degree in electrical engineering from the Helsinki University of Technology, Helsinki, Finland, in 2005 and 2007, respectively. She is currently a Professor with Xidian University, Xi'an, and a Visiting Professor with Aalto University, Espoo, Finland. She authored more than 150 peer-reviewed publications and solely authored two books. She is the inventor and the co-inventor of over 50 patents and PCT patent applications. Her research interests include trust, security and privacy, social networking, cloud computing, networking systems, and data mining. She also

serves as an Associate Editor of Information Sciences, Information Fusion, IEEE INTERNET OF THINGS JOURNAL, Journal of Network and Computer Applications (JNCA), and Security and Communication Networks. She is also a leading guest editor of many reputable journals, including

ACM Transactions on Multimedia Computing, Communications, and Applications (ACM TOMM), Future Generation Computer Systems (FGCS), IEEE SYSTEMS JOURNAL, and Mobile Networks and Applications (MONET). She has served as a steering, organization, and program committee member for over 70 international conferences.